

# Analysis of the bifurcating orbits on the route to chaos in confined thermal convection

Diego Angeli<sup>1</sup>, Arturo Pagano<sup>2</sup>,  
Mauro A. Corticelli<sup>1</sup>, Alberto Fichera<sup>2</sup>, and Giovanni S. Barozzi<sup>1</sup>

<sup>1</sup> University of Modena and Reggio Emilia, Department of Mechanical and Civil Engineering, Via Vignolese, 905, I-41125 Modena, Italy

(E-mail: [diego.angeli@unimore.it](mailto:diego.angeli@unimore.it))

<sup>2</sup> University of Catania, Department of Industrial and Mechanical Engineering Viale Andrea Doria, 6, I-95125 Catania, Italy

(E-mail: [apagano@diim.unict.it](mailto:apagano@diim.unict.it))

**Abstract.** Bifurcating thermal convection flows arising from a horizontal cylinder centred in a square-sectioned enclosure are studied numerically, with the aim of achieving a more detailed description of the sequence of transitions leading to the onset of chaos, and obtaining a more precise estimate of the critical values of the main system parameter, the Rayleigh number  $Ra$ . Only a value of the geometric aspect ratio  $A$  of the system is considered, namely  $A = 2.5$ , for which a period-doubling cascade was previously observed. Results give evidence of new and interesting features in the route to chaos, such as a window of quasiperiodic flow and the detection of high-order period orbits.

**Keywords:** Thermal convection, period-doubling cascade, quasi-periodicity, deterministic chaos.

## 1 Introduction

Buoyancy-induced flows in enclosures represents one of the most complete multi-scale coupled non-linear fluid flow problems. Their primary importance in the field of the study of bifurcations and chaos is due to the fact that they represent passive systems on which bifurcative dynamics easily show up, and, eventually, lead to relevant observations on the relationship between the onset of chaos and the transition from laminar to turbulent flow.

Many works have been carried out on the non-linear dynamics of thermal convection in basic enclosure configurations, such as the rectangular enclosures heated from below (the Rayleigh-Bénard problem) and from the side [1,2] (the “vertical enclosure” case), and, more recently, the horizontal annulus between two coaxial cylinders [3]. Fewer works dealt with more complex geometrical and thermal configurations [4–6]. Nevertheless, from a theoretical and practical standpoint, the interest in this topic is growing continuously.



The physical system considered in the present study is the cavity formed by an infinite square parallelepiped with a centrally placed cylindrical heating source. The system is approximated to its 2D transversal square section containing a circular heat source, as sketched in Fig. 1. The temperature of both enclosure and cylinder is assumed as uniform, the cylindrical surface being hotter than the cavity walls. Thus, the leading parameter of the problem is the Rayleigh number  $Ra$ , based on the gap width  $H$ , expressing the temperature difference in dimensionless terms. Another fundamental parameter is the Prandtl number, fixed for this study at a value  $Pr = 0.7$ , representative of air at environmental conditions.

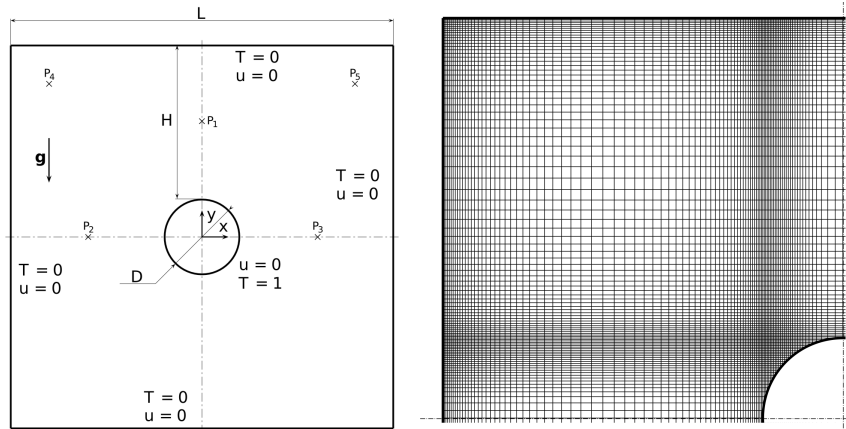


**Fig. 1.** Left: schematic of the system under consideration; (×) symbols indicate locations of the sampling points. Right: quadrant of the computational grid.

From the standpoint of thermofluids, the convective system in Fig. 1 is particularly interesting, since, due to the curvature of the cylindrical differentially heated surfaces, its phenomenology encompasses the features of both the Rayleigh-Bénard and the vertical enclosure cases. As soon as a temperature difference is imposed between the cylinder and the enclosure, fluid motion ensues immediately in the vicinity of the horizontal midplane, where the cylindrical walls are substantially vertical. On the other hand, the fluid in the top part of the enclosure is subject to an unstable vertical gradient, as in the Rayleigh-Bénard problem, while vertical boundary layers are invariably forming at the enclosure sidewalls. The combination of these situations in a single problem produces a variety of flow configurations and transition phenomena.

Previous studies [5,6] already unfolded different scenarios on the route to chaos of the system considered here, depending on its aspect ratio  $A = L/H$ . Accurate numerical investigations carried out for two  $A$ -values,  $A = 2.5$  and  $A = 5$ , revealed the existence of a period-doubling scenario following a Hopf bifurcation for  $A = 2.5$ , and a transition to chaos via a symmetry-breaking pattern followed by a blue-sky bifurcation for  $A = 5$  [6].

The aim of the present work is to achieve a deeper insight into the series of bifurcations for the case  $A = 2.5$ , in virtue of a wider set of numerical simulations performed by refining the step of the bifurcation parameter  $Ra$ . Particular attention has been devoted to the analysis of the stretching and folding attitudes of specific regions of the system attractor in proximity of the  $Ra$ -values corresponding to the period doubling bifurcation points, and in the chaotic range.

Numerical predictions are carried out by means of a specifically developed finite-volume code. Successive bifurcations of the low- $Ra$  fixed point solution are followed for increasing  $Ra$ . To this aim, time series of the state variables (velocity components and temperature), are extracted in 5 locations represented in Fig. 1 by points P1 to P5. Nonlinear dynamical features are described by means of phase-space representations, power spectra of the computed time series, and of Poincaré maps.

## 2 Problem statement and methods

The problem is stated in terms of the incompressible Navier-Stokes formulation, under the Boussinesq approximation. The governing equations (continuity, momentum and energy) are tackled in their non-dimensional form:

$$\nabla \cdot \mathbf{u} = 0 \quad (1)$$

$$\frac{\partial \mathbf{u}}{\partial t} + \mathbf{u} \cdot \nabla \mathbf{u} = -\nabla p + \frac{Pr^{1/2}}{Ra^{1/2}} \nabla^2 \mathbf{u} + T \hat{\mathbf{g}} \quad (2)$$

$$\frac{\partial T}{\partial t} + \mathbf{u} \cdot \nabla T = \frac{1}{(RaPr)^{1/2}} \nabla^2 T \quad (3)$$

where  $t$ ,  $\mathbf{u}$ ,  $p$  and  $T$  represent the dimensionless time, velocity vector, pressure and temperature, respectively, and  $\hat{\mathbf{g}}$  is the gravity unit vector. A value  $Pr = 0.7$  is assumed for air. Boundary conditions for  $T$  and  $\mathbf{u}$  are reported in Fig. 1.

Detailed descriptions of the adopted numerical techniques and of discretization choices are found in previous works [5,7]. A detail of the computational grid is shown in Fig. 1. In order to analyze the system dynamics in the vicinity of bifurcation points,  $Ra$  was increased monotonically with suitable steps, each simulation starting from the final frame of the preceeding one. All the simulations were protracted until a fixed dimensionless time span was covered, large enough for an asymptotic flow to be attained.

## 3 Results and discussion

In previous studies [5,6] a preliminary analysis of the system with  $A = 2.5$  reported the birth of chaotic behaviours for  $Ra$  greater than  $Ra = 2.0 \cdot 10^5$ . In particular, power spectral density distributions, attractor representations and

Poincaré maps were used to give a clear evidence of a basic period doubling route to chaos. In particular, it was shown that the flow is characterised by two fundamental harmonics at  $Ra = 1.7 \cdot 10^5$ , four harmonics at  $Ra = 1.8 \cdot 10^5$  and eight at  $Ra = 1.9 \cdot 10^5$ , whereas chaos was observed at  $Ra = 2.0 \cdot 10^5$ .

Given the great theoretical and practical importance of an accurate determination of the bifurcating behaviour of the flow, deeper analyses have been performed by refining the step of numerical simulation of the range of interest of the Rayleigh number. As described in the following, two main results have been obtained: (i) the identification of a window of quasiperiodic flow; (ii) the identification of three further period doublings precluding appearance of chaos.

### 3.1 Window of quasiperiodic flow

Several simulations performed in the range  $Ra = 1.7 \div 1.9 \cdot 10^5$  have been found to be characterised by a well defined quasiperiodic behaviour. Again, the observation of this result has been performed both in the frequency domain and in the state space.

Fig. 2 reports the PSDs of the variables simulated at point P1 for the case at  $Ra = 176875$ , in (a) for the horizontal velocity component  $u$ , in (b) for the vertical velocity component  $v$  and in (c) for the temperature  $T$ .

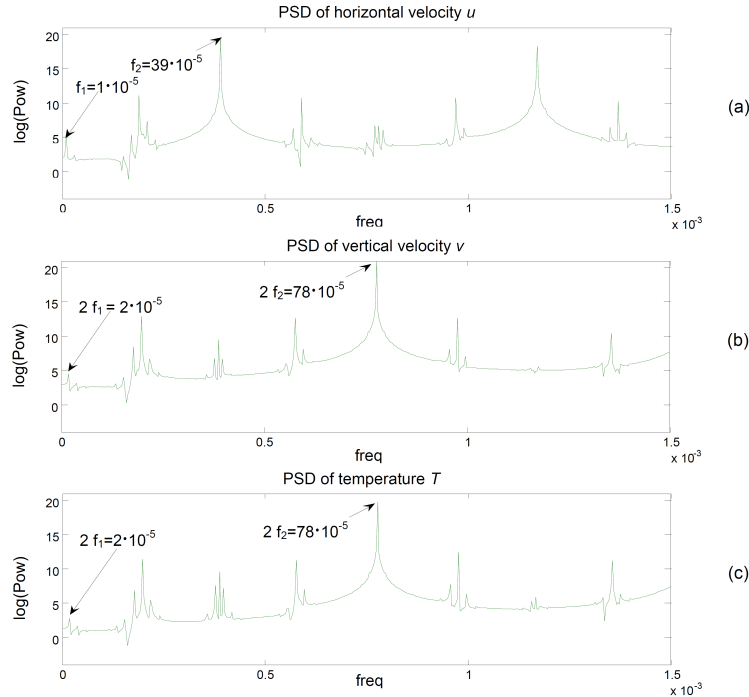


**Fig. 2.** PSDs of the simulated state variables at point P1 for the quasiperiodic case at  $Ra = 176875$ : (a) horizontal velocity  $u$ ; (b) vertical velocity  $v$ ; (c) temperature  $T$ .

The following interesting observations can be drawn from the analysis of the three plots of Fig. 2:

- the PSDs of  $v$  and  $T$  are mainly the same, as a consequence of the vertical character of the buoyancy-driven flow that determines the dynamics of the thermal and velocity field;
- the quasiperiodic behaviour finds a clear expression in the excitation of two independent frequencies, reported in the figures, and of bands formed by their linear harmonic combinations;
- the two dominant frequencies of  $v$  and  $T$ , exactly double those of the horizontal velocity  $u$ , as a direct consequence of the vertical symmetry of the domain.

Fig. 3 reports the phase plots for the simulation at point P1 for the case at  $Ra = 176875$ , i.e. for the same quasiperiodic dynamic discussed in Fig. 2. Plot (a) reports the whole toroidal attractor, whereas plot (b) allows for a deeper observation of the narrow toroidal structure of the attractor itself. Finally, plots (c), (d) and (e) reports the Poincaré map obtained by sectioning the attractor with the planes orthogonal to each of the axis in correspondence of the mean value of respective variable in the considered observation window. From the analysis of the plots in Fig. 3 it is possible to draw a further clear proof of the existence of the quasiperiodic behaviour, manifested in the state space by the torus and in the Poincaré maps by the elliptical traces. Notice that in plot (c) two partly superimposed elliptical traces appears as a consequence of the intersection of the two branches of the torus in the chosen Poincaré plane.

It is worthy to mention that further analyses, omitted here for brevity, revealed that the quasiperiodic torus appears  $Ra = 1.740 \cdot 10^5$ , bifurcating from the stable limit cycle which represents the solution at  $Ra = 1.735 \cdot 10^5$ , while it disappears, for  $Ra = 1.795 \cdot 10^5$ , giving rise to the period-doubling route described in the following. Such observations contribute to shed light on the proper bifurcation path in the range  $Ra = 1.740 \div 1.795 \cdot 10^5$ , which therefore redefines the simple period doubling assumed in [6].

### 3.2 High order period doublings

A further refinement of the  $Ra$  steps of the simulation in the range  $Ra = 1.9 \div 2.0 \cdot 10^5$  allowed for the determination the critical values of  $Ra$  at which higher order period doublings occur. In particular, the progressive increase from  $Ra = 1.8 \cdot 10^5$ , for which a period 8 limit cycle exists, it has been possible to determine the birth of the limit cycles characterised by 16, 32, 64 and even 128 periods, which anticipate the appearance of chaos.

From the analysis of the extensive simulations performed for very narrow step of  $Ra$  in the range  $Ra = 1.9 \div 2.0 \cdot 10^5$ , completed with the observation of the window of quasiperiodic behaviour, it has been possible to summarise the complete bifurcation path from period-2 limit cycle to chaos according to the limits reported in Tab. 3.2. There, the notation introduced in [3] is used to identify the different flow regimes.

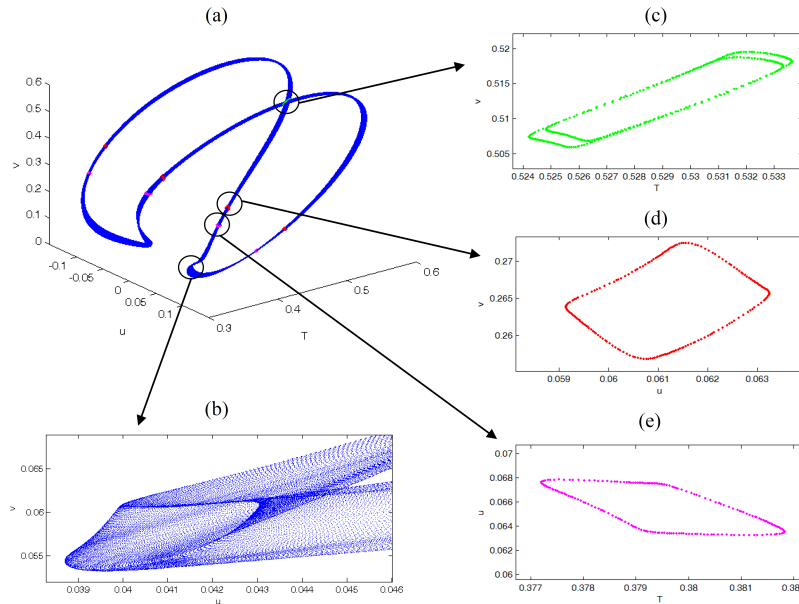


**Fig. 3.** Phase plots of the quasiperiodic dynamical behaviour at point  $P_1$  for  $Ra = 176875$  : (a) attractor in the state space  $T-u-v$ ; (b) particular evidencing the structure of the narrow torus; (c), (d), (e) Poincaré maps.

	$P_1$	$QP_2$	$P_2$	$P_4$	$P_8$
$Ra \cdot 10^{-5}$	$\leq 1.735$	$1.74 \div 1.79$	$1.795 \div 1.8975$	$1.898 \div 1.9367$	$1.93675 \div 1.94730$
	$P_{16}$	$P_{32}$	$P_{64}$	$N$	
$Ra \cdot 10^{-5}$	$1.94735 \div 1.9495$	$1.94955 \div 1.94985$	$1.9499$	$> 1.95$	

**Table 1.** Sequence of flow regimes encountered and correspondent ranges of  $Ra$ .

Fig. 4 reports the Poincaré maps for some characteristic values of the Rayleigh number falling within the ranges of limit cycles of high-order period (from  $P_4$  to  $P_{64}$ ) as well as for one value in the chaotic range,  $Ra = 1.9625 \cdot 10^5$ . In each map it is possible to observe the existence of four clusters of points, each of which can be considered generated by the four intersections of the original  $P_1$  limit cycle existing for  $Ra \leq 1.735 \cdot 10^5$ . In order to achieve a deeper detail on the phenomenon, the encircled clusters in Fig. 4 are reported in Fig. 5, where the series of doubling of each point can be better observed. As a final remark, it is possible to observe that the period doubling bifurcation path is responsible for the birth of bands in the chaotic attractor, characterised by a marked attitude to stretching and folding typical of fractal sets, as it can be deduced by the ordered distribution of the intersections in the Poincaré maps.

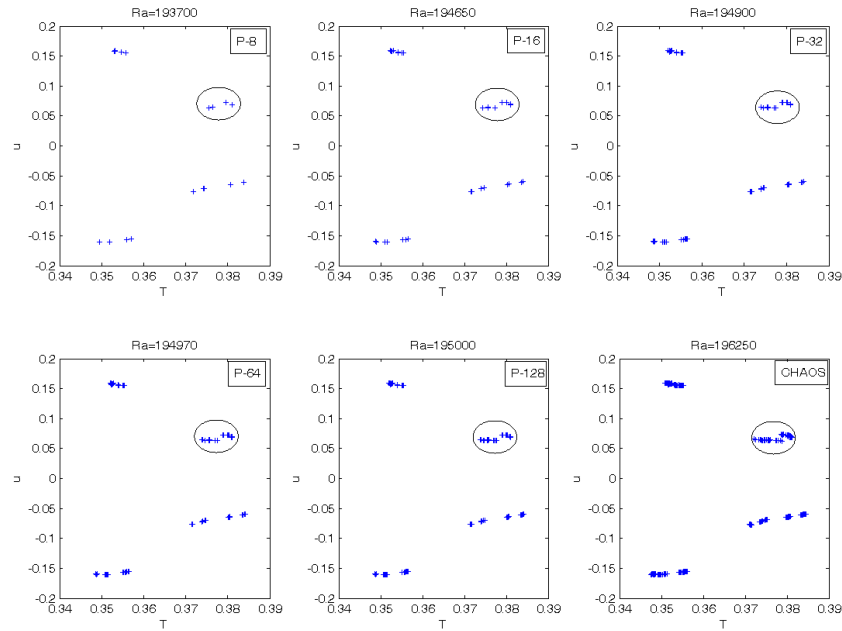


**Fig. 4.** Poincaré maps for characteristic  $Ra$ -values, for limit cycles of high-order period (from  $P_4$  to  $P_{64}$ ) and chaos.

#### 4 Concluding remarks

The sequence of bifurcations leading to deterministic chaos in natural convection from a horizontal cylindrical source, centred in a square enclosure of aspect ratio  $A = 2.5$ , was analysed in detail by numerical means.

The set of long term simulations revealed further remarkable aspects of the route to chaos of the system, for increasing the main parameter  $Ra$ . In first instance, a window of quasiperiodic behaviour was observed over a wide range of  $Ra$ -values, originating from the first limit cycle and giving rise to the subsequent the period-doubling cascade.

Furthermore, the refinement of the parameter range allowed for the detection of additional stages in the sequence of period doublings of the system, up to the observation of a  $P_{64}$  orbit, before the final appearance of chaos.

#### References

- 1.K. T. Yang. Transitions and bifurcations in laminar buoyant flows in confined enclosures. *ASME Journal of Heat Transfer*, 110:1191–1204, 1988.
- 2.P. Le Quééré. Onset of unsteadiness, routes to chaos and simulations of chaotic flows in cavities heated from the side: a review of present status. In G. F. Hewitt, editor, *Proceedings of the Tenth International Heat Transfer Conference*, volume 1, pages 281–296, Brighton, UK, 1994. Hemisphere Publishing Corporation.

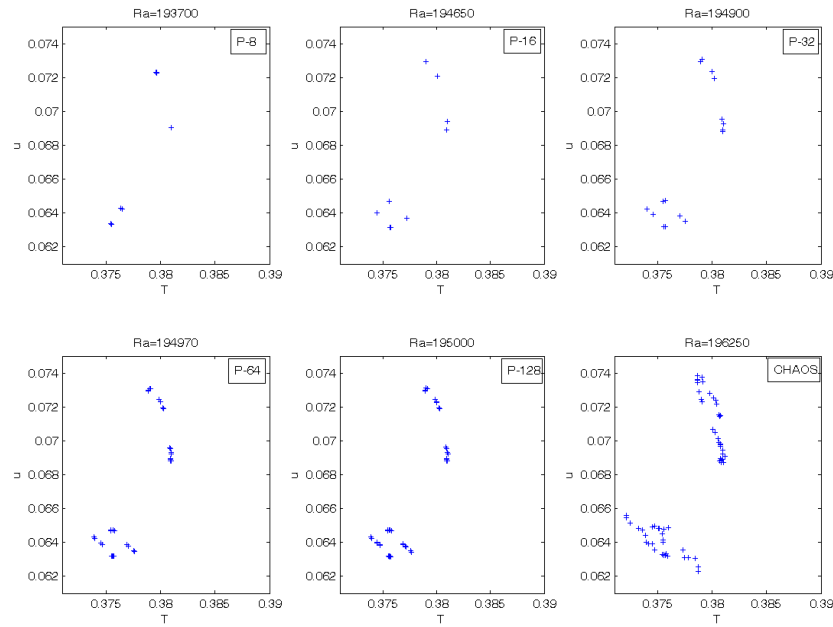


**Fig. 5.** Details of the encircled clusters of points in the Poincaré maps of Fig. 4.

- 3.D. Angeli, G. S. Barozzi, M. W. Collins, and O. M. Kamiyo. A critical review of buoyancy-induced flow transitions in horizontal annuli. *International Journal of Thermal Sciences*, 49:2231–2492, 2010.
- 4.G. Desrayaud and G. Lauriat. Unsteady confined buoyant plumes. *Journal of Fluid Mechanics*, 252:617–646, 1998.
- 5.D. Angeli, A. Pagano, M. A. Corticelli, A. Fichera, and G. S. Barozzi. Bifurcations of natural convection flows from an enclosed cylindrical heat source. *Frontiers in Heat and Mass Transfer*, 2:023003, 2011.
- 6.D. Angeli, A. Pagano, M.A. Corticelli, and G.S. Barozzi. Routes to chaos in confined thermal convection arising from a cylindrical heat source. *Chaotic Modeling and Simulation*, 1:61–68, 2011.
- 7.D. Angeli, P. Levoni, and G. S. Barozzi. Numerical predictions for stable buoyant regimes within a square cavity containing a heated horizontal cylinder. *International Journal of Heat and Mass Transfer*, 51:553–565, 2008.